PHYSICAL REVIEW D **83,** 034023 (2011)

Possible resolution of the $B \to \pi\pi$, πK puzzles

Hsiang-nan Li[1,*] and Satoshi Mishima[2,†]

[1]*Institute of Physics, Academia Sinica, Taipei, Taiwan 115, Republic of China*
and Department of Physics, Tsing-Hua University, Hsinchu, Taiwan 300, Republic of China
and Department of Physics, National Cheng-Kung University, Tainan, Taiwan 701, Republic of China
[2]*Theory Group, Deutsches Elektronen-Synchrotron DESY, 22607 Hamburg, Germany*

(Received 16 January 2009; revised manuscript received 29 November 2010; published 22 February 2011)

We show that there exist uncanceled soft divergences in the k_T factorization for nonfactorizable amplitudes of two-body nonleptonic B meson decays, similar to those identified in hadron hadroproduction. These divergences can be grouped into a soft factor using the eikonal approximation, which is then treated as an additional nonperturbative input in the perturbative QCD formalism. Viewing the special role of the pion as a $q\bar{q}$ bound state and as a pseudo Nambu-Goldstone boson, we postulate that the soft effect associated with it is significant. This soft factor enhances the nonfactorizable color-suppressed tree amplitudes, such that the branching ratios $B(\pi^0\pi^0)$ and $B(\pi^0\rho^0)$ are increased under the constraint of the $B(\rho^0\rho^0)$ data, the difference between the direct CP asymmetries $A_{CP}(\pi^\mp K^\pm)$ and $A_{CP}(\pi^0 K^\pm)$ is enlarged, and the mixing-induced CP asymmetry $S_{\pi^0 K_S}$ is reduced. Namely, the known $\pi\pi$ and πK puzzles can be resolved simultaneously.

DOI: 10.1103/PhysRevD.83.034023 PACS numbers: 12.39.St, 12.38.Bx, 13.25.Hw

I. INTRODUCTION

The more precise data of the $B \to \pi\pi$, πK decays have sharpened the discrepancies with the theoretical predictions from the factorization approaches, such as the perturbative QCD (PQCD) approach based on the k_T factorization theorem [1,2]. The observed $B^0 \to \pi^0\pi^0$ branching ratio [3] remains several times larger than the naive expectation. The direct CP asymmetry of the $B^\pm \to \pi^0 K^\pm$ decays differs dramatically from that of the $B^0 \to \pi^\mp K^\pm$ decays. There is a deviation between the extractions of the standard model parameter $\sin(2\phi_1)$ from the penguin-dominated $B^0 \to \pi^0 K_S$ modes and from the tree-dominated $b \to c\bar{c}s$ modes. All these discrepancies are closely related to the color-suppressed tree amplitudes C [4]. The $B^0 \to \pi^0\rho^0$ branching ratios from PQCD and QCD factorization (QCDF), being sensitive to C, are also much lower than the data [5,6]. However, the estimate of C from PQCD is well consistent with the measured $B^0 \to \rho^0\rho^0$ branching ratio [7]. Proposals resorting to new physics [8] mainly resolve the πK puzzle without addressing the peculiar feature of C in the $\pi^0\pi^0$, $\pi^0\rho^0$, and $\rho^0\rho^0$ modes, while those to QCD effects are usually strongly constrained by the $\rho\rho$ data [9]. It indicates the difficulty of resolving the $\pi\pi$ and πK puzzles simultaneously.

The color-suppressed tree amplitude C seems to be an important but the least understood quantity in B meson decays. Viewing that all the puzzles appear in the C-sensitive quantities, we shall carefully investigate QCD effects on C, and their impact on the $B \to \pi\pi$, πK decays. Once a mechanism identified for C respects the conventional factorization theorem, it is unlikely to be a resolution due to the $B \to \rho\rho$ constraint mentioned above [7]. That is the reason the higher-order corrections calculated in QCDF [10], which obey the collinear factorization, cannot resolve the $\pi\pi$ puzzle. It has been pointed out by Collins and Qiu [11] that the k_T factorization breaks down in complicated QCD processes like high-p_T hadron hadroproduction because of the existence of soft gluons in the Glauber region. To factorize the collinear gluons associated with, say, one of the initial-state hadrons, one needs to eikonalize the valence quark lines to which the collinear gluons attach. Those eikonal lines, i.e., Wilson lines from another initial-state hadron and the final-state hadrons, should cancel in order to have the universality of the considered parton distribution function. However, the required cancellation is not exact in the k_T factorization, though it is in the collinear factorization. The k_T factorization still holds for simple processes like deeply inelastic scattering (DIS), which does not involve the Wilson lines from the other hadrons. The Glauber gluons have been included as a mode in the soft-collinear effective theory (SCET) recently [12].

The above observation provides a clue for resolving the $\pi\pi$ and πK puzzles. It is easy to see that a factorizable amplitude, involving only a B meson transition form factor, mimics simple DIS, and a nonfactorizable [13] amplitude, involving dynamics of three hadrons, mimics the complicated hadron hadroproduction. The k_T factorization for a factorizable B meson decay amplitude has been proved [14]. The k_T factorization for a nonfactorizable amplitude has not, though it has been widely employed in the PQCD analysis. Below we shall identify the residual infrared divergence in the k_T factorization for a nonfactorizable

*hnli@phys.sinica.edu.tw
†satoshi.mishima@desy.de

amplitude at one loop. Contrary to high-p_T hadron hadroproduction, this residual infrared divergence can be factorized into a soft factor in two-body nonleptonic B meson decays, following the procedure in [15], such that the universality of a k_T-dependent meson wave function is restored. A nonfactorizable amplitude then remains calculable in the PQCD approach after parametrizing the soft factor. The color-suppressed tree amplitude C receives a small factorizable contribution, so the soft effect on a nonfactorizable amplitude could be significant for C.

In Sec. II we show the existence of residual infrared divergences caused by Glauber gluons in a nonfactorizable emission diagram. It is explained by means of contour deformation why Glauber gluons, which do not meet the criteria of eikonalization in usual QCD processes, can be factorized from two-body nonleptonic B meson decays. It is emphasized that the Glauber divergences do not appear in the collinear factorization, such as the QCDF approach. In Sec. III we prove the factorization of the Glauber divergences into a soft factor up to all orders, and derive its definition in terms of nonlocal Wilson operators. We then investigate the numerical impact of the soft factor on two-body nonleptonic B meson decays in Sec. IV, and demonstrate that the $B \to \pi\pi$ and πK puzzles mentioned above can be resolved. Section V contains the conclusion.

II. EIKONALIZATION OF GLAUBER GLUONS

Consider the $B(P_B) \to M_1(P_1)M_2(P_2)$ decay, where $P_{B,1,2}$ represent the momenta of the B, M_1, and M_2 mesons, respectively. For convenience, we choose P_1 (P_2) in the plus (minus) direction. Start with the leading-order (LO) nonfactorizable emission diagram in Fig. 1(a) resulting from the operator O_2 [16], where the parton momenta k, k_1, and k_2 have been labeled. We add a radiative gluon of momentum l collinear to P_2, which is emitted by the valence quark in M_2. The attachment of the radiative gluon to the b quark line shown in Fig. 2(a) leads to a Wilson line from infinity to the origin, i.e., the weak vertex. This piece is factorized in color flow by itself with the color factor C_F. The attachment to the hard gluon in Fig. 2(b) generates two Wilson lines, one of which runs from the position z_2 of the valence antiquark in M_2 to infinity [17]. The attachments to the virtual antiquark in Fig. 2(c) and to the valence quark in the M_1 meson in Fig. 2(d) also generate the Wilson line

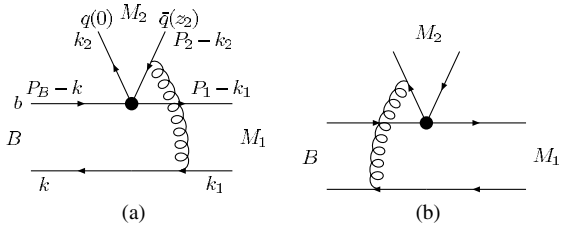

FIG. 1 (color online). LO diagrams for a nonfactorizable amplitude.

running from z_2 to infinity. The combination of these three pieces with the same Wilson line is factorized in color flow. As to the next-to-leading-order (NLO) two-particle reducible diagrams, such as the self-energy correction to the valence quark in Fig. 3(a) and the gluon exchange between the valence quark and the valence antiquark in Fig. 3(b), their factorization into the M_2 meson wave function is straightforward [17].

The detail of the above treatment is similar to that presented in [14,17] for the pion form factor and the B meson transition form factor, which leads to the k_T-dependent M_2 meson wave function,

$$\Phi_{M_2}(x_2, k_{2T}) = \int \frac{dz_2^+ d^2 z_{2T}}{(2\pi)^3} \exp(-ix_2 P_2^- z_2^+ + i\mathbf{k}_{2T}\cdot\mathbf{z}_{2T}) \times \langle 0|\bar{q}(z_2)\gamma_5 \not{n}_+ W_+(z_2^+, \mathbf{z}_{2T}; \infty)^\dagger \times W_+(0, \mathbf{0}_T; \infty) q(0)|M_2(P_2)\rangle, \quad (1)$$

with the coordinate $z_2 = (z_2^+, 0, \mathbf{z}_{2T})$ of the valence antiquark and the dimensionless vector $n_+ = (1, 0, \mathbf{0}_T)$ being along the light cone. The path-ordered exponential W_+ collects the Wilson lines mentioned above:

$$W_+(z^+, \mathbf{z}_T; \infty) = P\exp\left[-ig\int_0^\infty d\lambda n_+ \cdot A(z + \lambda n_+)\right]. \quad (2)$$

A vertical link to connect the two Wilson lines $W_+(z_2^+, \mathbf{z}_{2T}; \infty)^\dagger$ and $W_+(0, \mathbf{0}_T; \infty)$ at infinity is understood [18,19].

The other attachments shown in Figs. 2(e) and 2(f) and the second piece from Fig. 2(b) should cancel in order to have the universality of the M_2 meson wave function in Eq. (1). We shall point out that it is not the case, and the sum of the above three pieces gives a residual infrared divergence. First, we justify the eikonalization of the soft spectator in Fig. 2(e), which demands the inclusion of the NLO diagram in Fig. 4(a). Figure 4(a) contains the four denominators

$$[(P_2 - k_2 + l)^2 + i\epsilon][(k - k_1 + l)^2 + i\epsilon] \times [(k + l)^2 + i\epsilon](l^2 + i\epsilon), \quad (3)$$

with the loop momentum l, which define the following poles in the l^- plane:

$$l^- = -(P_2^- - k_2^-) + \frac{|\mathbf{l}_T - \mathbf{k}_{2T}|^2}{2l^+} - i\epsilon(+i\epsilon), \quad (4)$$

$$l^- = -k^- + \frac{|\mathbf{l}_T - \mathbf{k}_{1T} + \mathbf{k}_T|^2}{2(l^+ - k_1^+ + k^+)} + i\epsilon(+i\epsilon), \quad (5)$$

$$l^- = -k^- + \frac{|\mathbf{l}_T + \mathbf{k}_T|^2}{2(l^+ + k^+)} - i\epsilon(-i\epsilon), \quad (6)$$

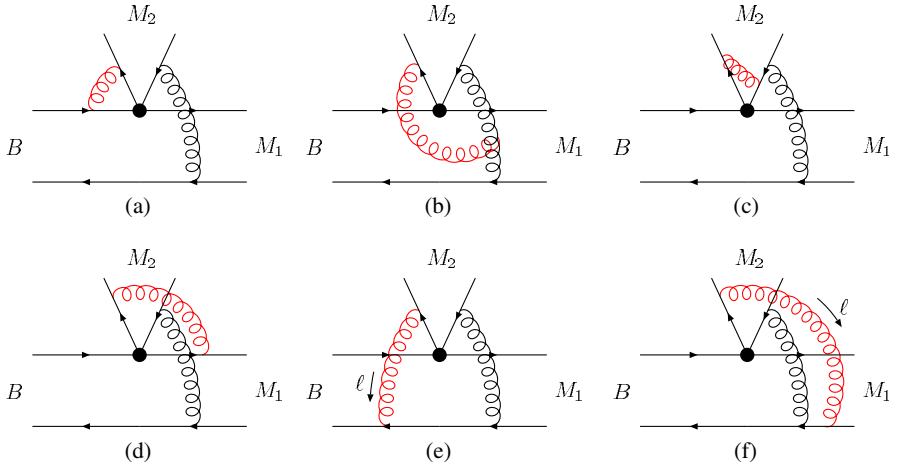

FIG. 2 (color online). NLO diagrams for Fig. 1(a) that are relevant to the factorization of the M_2 meson wave function.

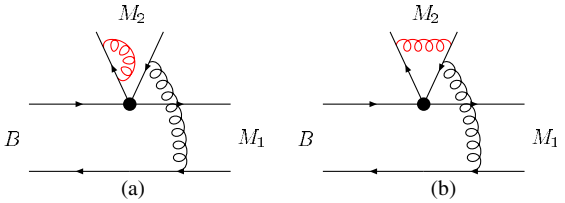

FIG. 3 (color online). Two-particle reduced NLO diagrams for the M_2 meson wave function.

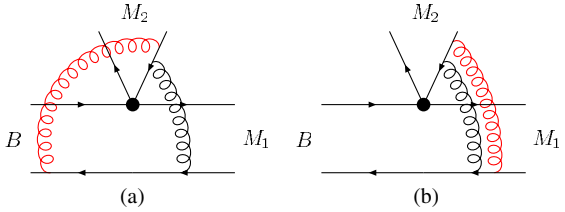

FIG. 4 (color online). NLO diagrams that do not contribute the Glauber divergence.

$$l^- = \frac{l_T^2}{2l^+} - i\epsilon(+i\epsilon), \tag{7}$$

for the range of $0 < l^+ < k_1^+ - k^+$ ($-k^+ < l^+ < 0$). Here the inequality $k_1^+ > k^+$ has been assumed for convenience. The first pole, being the furthest one, does not pinch the contour of l^- actually. The two poles in Eqs. (5) and (6) demand that the contour goes through the region of $l^- \sim \Lambda_{\rm QCD}$ for the soft spectator momentum $k^\mu \sim \Lambda_{\rm QCD}$ and the small transverse loop momentum $l_T \sim \Lambda_{\rm QCD}$, $\Lambda_{\rm QCD}$ being the QCD scale. This observation does not depend on the order of magnitude of the fourth pole. There is no pinched singularity for $l^+ > (k_1^+ - k^+)$ and for $l^+ < -k^+$, because all the poles of l^- are in the same half plane.

Figure 2(e) contains the five denominators

$$[(k_2 + l)^2 + i\epsilon][(P_2 - k_2 - k + k_1 - l)^2 + i\epsilon] \times [(k - k_1 + l)^2 + i\epsilon][(k + l)^2 + i\epsilon](l^2 + i\epsilon). \tag{8}$$

Similarly, there is no pinched singularity for $l^+ > (k_1^+ - k^+)$ and for $l^+ < -k^+$. We consider the poles

$$l^- = -k_2^- + \frac{|\mathbf{l}_T + \mathbf{k}_{2T}|^2}{2l^+} - i\epsilon(+i\epsilon), \tag{9}$$

$$l^- = P_2^- - k_2^- - k^- + \frac{|\mathbf{l}_T + \mathbf{k}_{2T} - \mathbf{k}_{1T} + \mathbf{k}_T|^2}{2(l^+ - k_1^+ + k^+)} + i\epsilon(+i\epsilon), \tag{10}$$

$$l^- = -k^- + \frac{|\mathbf{l}_T - \mathbf{k}_{1T} + \mathbf{k}_T|^2}{2(l^+ - k_1^+ + k^+)} + i\epsilon(+i\epsilon), \tag{11}$$

$$l^- = -k^- + \frac{|\mathbf{l}_T + \mathbf{k}_T|^2}{2(l^+ + k^+)} - i\epsilon(-i\epsilon), \tag{12}$$

$$l^- = \frac{l_T^2}{2l^+} - i\epsilon(+i\epsilon), \tag{13}$$

for $0 < l^+ < k_1^+ - k^+$ ($-k^+ < l^+ < 0$). The poles in Eqs. (9) and (10) are far from the origin by $l^- \sim O(m_B)$ due to the large momenta k_2 and $P_2 - k_2$, m_B being the B meson mass, so they do not pinch the contour of l^-. The other three poles in Eqs. (5)–(7) identical to those in Eqs. (10), (11), and (13), respectively, for both ranges of $0 < l^+ < k_1^+ - k^+$ and $-k^+ < l^+ < 0$, demand that the contour goes through the region of $l^- \sim \Lambda_{\rm QCD}$.

We focus on the soft divergence from $l^+ \to 0$ and $l_T \to 0$, since the infrared finite piece contributes to the NLO hard kernel. Picking up the poles of $O(\Lambda_{\rm QCD})$ in Eqs. (5) and (11) for $0 < l^+ < k_1^+ - k^+$, the l^- dependence in $(P_2 - k_2 + l)^2$, $(k_2 + l)^2$, and $(P_2 - k_2 - k + k_1 - l)^2$ is negligible. Picking up the poles of $O(\Lambda_{\rm QCD})$

in Eqs. (6) and (12) for $-k^+ < l^+ < 0$, the l^- dependence is also negligible. Ignoring $k_{2T}^2 \sim O(\Lambda_{\rm QCD}^2)$ in $(P_2 - k_2 + l)^2$ and $(k_2 + l)^2$, Figs. 2(e) and 4(a) have the same amplitudes except a sign difference, which is attributed to the emissions of the radiative gluon by the valence quark and by the valence antiquark in M_2. Because of this soft cancellation in the pinched configuration, only the $O(m_B)$ poles in Eqs. (9) and (10) for the range $0 < l^+ < k_1^+ - k^+$ are relevant. It implies that the contour of l^- in Fig. 2(e) can be deformed across the $O(\Lambda_{\rm QCD})$ poles, and always remains at least of $O(m_B)$. That is, for a gluon radiated from the energetic M_2 meson, we can consider only a collinear divergence, instead of a soft divergence, if infrared divergences are concerned. We then have the hierarchy

$$k^+ l^- \sim O(\Lambda_{\rm QCD} m_B) \gg |\mathbf{l}_T + \mathbf{k}_T|^2 \sim O(\Lambda_{\rm QCD}^2), \quad (14)$$

for the denominator $(k + l)^2$. Therefore, the eikonal approximation applies to the soft spectator on the B meson side, giving the propagator $1/(n_+ \cdot l + i\epsilon)$.

The loop integral associated with Fig. 2(e) is then written as

$$I_E = C_F \int \frac{d^4 l}{(2\pi)^4} \mathrm{tr}\Big[\cdots \frac{-i(P_2 - \not{k}_2 - \not{k} + \not{k}_1 - \not{l})}{(P_2 - k_2 - k + k_1 - l)^2 + i\epsilon} \times (-ig\gamma_\beta)\gamma_5 \not{P}_2 (-ig\gamma_\alpha) \frac{i(\not{k}_2 + \not{l})}{(k_2 + l)^2 + i\epsilon}\Big] \times \frac{-i}{(k - k_1 + l)^2 + i\epsilon} \frac{-g n_+^\alpha}{n_+ \cdot l + i\epsilon} \frac{-i}{l^2 + i\epsilon}, \quad (15)$$

where the ... denotes the rest of the integrand, and $\gamma_5 \not{P}_2$ comes from the twist-2 structure of the M_2 meson wave function. Combining Figs. 2(f) and 4(b) with the cancellation of the ordinary soft divergences between them, we justify the eikonal approximation for the spectator propagator $1/[(k_1 - l)^2 + i\epsilon]$, which gives $1/(-n_+ \cdot l + i\epsilon)$. The second piece from Fig. 2(b) contains the Wilson line running from the position of the spectator in the M_1 meson to infinity, i.e., the eikonal propagator $1/(-n_+ \cdot l + i\epsilon)$. This piece with the color factor $N_c/2$, together with Fig. 2(f) with the color factor $-1/(2N_c)$, leads to the loop integral the same as Eq. (15) with the color factor C_F, but with $1/(n_+ \cdot l + i\epsilon)$ being replaced by $1/(-n_+ \cdot l + i\epsilon)$. Employing the principal-value prescription,

$$\frac{1}{n_+ \cdot l + i\epsilon} + \frac{1}{-n_+ \cdot l + i\epsilon} = -2\pi i \delta(l^-), \quad (16)$$

we identify a NLO residual soft divergence from the Glauber region with $l^- = 0$, which seems to violate the universality of the M_2 meson wave function.

The spectator propagators in Fig. 4 can also be replaced by the Wilson line in the direction of n_+ for collecting the Glauber divergences, if there are any. The eikonalization is achieved by deforming the l^- contour under the soft cancellation observed above. We then examine the l^+ poles from the denominators in Eq. (3) with $l^- = 0$ being demanded by Eq. (16):

$$l^+ = \frac{|\mathbf{l}_T - \mathbf{k}_{2T}|^2}{2(P_2^- - k_2^-)} - i\epsilon, \quad (17)$$

$$l^+ = k_1^+ - k^+ + \frac{|\mathbf{l}_T - \mathbf{k}_{1T} + \mathbf{k}_T|^2}{2k^-} - i\epsilon. \quad (18)$$

It is seen that both l^+ poles are located in the lower half plane, namely, Fig. 4 does not contribute to the Glauber divergences. Figure 4 generates only the ordinary soft divergences from the region of the loop momentum $l^\mu \equiv (l^+, l^-, l_T) \sim (\Lambda_{\rm QCD}, \Lambda_{\rm QCD}, \Lambda_{\rm QCD})$ [20]. The effect from these ordinary soft gluons has been analyzed and found to be negligible in two-body nonleptonic B meson decays, though it may be significant in D meson decays [21].

The l^+ poles from Fig. 2(e) in Eq. (8) with $l^- = 0$ are given by

$$l^+ = \frac{|\mathbf{l}_T + \mathbf{k}_{2T}|^2}{2k_2^-} - i\epsilon, \quad (19)$$

$$l^+ = k_1^+ - k^+ - \frac{|\mathbf{l}_T + \mathbf{k}_{2T} - \mathbf{k}_{1T} + \mathbf{k}_T|^2}{2(P_2^- - k_2^- - k^-)} + i\epsilon, \quad (20)$$

$$l^+ = k_1^+ - k^+ + \frac{|\mathbf{l}_T - \mathbf{k}_{1T} + \mathbf{k}_T|^2}{2k^-} - i\epsilon, \quad (21)$$

in which only the first pole is of $O(\Lambda_{\rm QCD}^2/m_B)$. As long as k_1^+ is of or greater than $O(\Lambda_{\rm QCD})$, we can deform the contour of l^+, such that l^+ remains $O(\Lambda_{\rm QCD})$, and the hierarchy

$$k_2^- l^+ \sim O(m_B \Lambda_{\rm QCD}) \gg |\mathbf{l}_T + \mathbf{k}_{2T}|^2 \sim O(\Lambda_{\rm QCD}^2) \quad (22)$$

holds. The valence quark carrying the momentum $k_2 + l$ in Eq. (15) can then be eikonalized into $n_{-\alpha}/(n_- \cdot l + i\epsilon)$ with the vector $n_- = (0, 1, \mathbf{0}_T)$. The Glauber divergence associated with Fig. 1(a) is collected by

$$I_a^{(1)} = g^2 C_F \int \frac{d^4 l}{(2\pi)^4} \mathrm{tr}\Big[\cdots \frac{-i(P_2 - \not{k}_2 - \not{k} + \not{k}_1 - \not{l})}{(P_2 - k_2 - k + k_1 - l)^2 + i\epsilon} \times (-ig\gamma_\beta)\gamma_5 \not{P}_2\Big] \frac{-i}{(k - k_1 + l)^2 + i\epsilon} \frac{1}{l^+ + i\epsilon} \times \frac{-i}{-l_T^2 + i\epsilon} 2\pi i \delta(l^-), \quad (23)$$

where the gluon propagator proportional to $1/l_T^2$ explicitly indicates that the infrared divergence we have identified arises from the Glauber region.

It is stressed that Eq. (23), derived from Fig. 2(e), contains the Glauber divergence associated with Fig. 1(b) as well: the left (right) gluon in Fig. 2(e) may become hard (soft) in some region of the loop momentum l. We started with the eikonalization of the left gluon in Fig. 2(e),

implying the attempt to isolate the Glauber divergence associated with Fig. 1(a). For consistency and for avoiding double counting, we close the contour in the lower half plane of l^+, and pick up only the pole $l^+ = 0 - i\epsilon$ from the eikonal propagator $1/l^+$, which corresponds to the $O(\Lambda^2_{\rm QCD}/m_B)$ pole in Eq. (19). Another pole in Eq. (21), corresponding to the on-shell right gluon, contributes to the Glauber divergence associated with Fig. 1(b). Equation (23) is then simplified into

$$I_a^{(1)} \approx i\frac{\alpha_s}{\pi} C_F \int \frac{d^2 l_T}{l_T^2} \mathcal{M}_a^{(0)}(\mathbf{l}_T), \tag{24}$$

where $\mathcal{M}_a^{(0)}$ denotes the LO amplitude from Fig. 1(a), and the imaginary logarithmic divergence is explicit.

The Glauber divergence may not cause trouble, if the LO amplitude $\mathcal{M}^{(0)}$ is real. Expanding the decay width up to NLO, we have

$$|\mathcal{M}|^2 = |\mathcal{M}^{(0)}|^2 + 2\,{\rm Re}[\mathcal{M}^{(0)}\mathcal{M}^{(1)*}]. \tag{25}$$

According to Eq. (24), the Glauber divergence will be purely imaginary, if $\mathcal{M}^{(0)}$ is real, so it does not survive in the second term ${\rm Re}[\mathcal{M}^{(0)}\mathcal{M}^{(1)*}]$. That is, the Glauber divergence does not exist in the collinear factorization. The absence of the Glauber divergence has been shown up to two loops in the collinear factorization for hadron hadroproduction [11]. On the contrary, $\mathcal{M}^{(0)}$ is complex in the k_T factorization, since partons carry transverse momenta, and internal lines go on mass shell at finite momentum fractions [22]. Thus, the Glauber divergence contributes to ${\rm Re}[\mathcal{M}^{(0)}\mathcal{M}^{(1)*}]$ in the PQCD approach to two-body nonleptonic B meson decays. In the QCDF calculation [10] based on SCET [23], the virtual antiquark line in Fig. 2 has been shrunk to a point, because this line is believed to be more off shell than the hard gluon. The pole in Eq. (20) then disappears, and the other two in Eqs. (19) and (21) are located in the lower half plane of l^+. As a consequence, the Glauber divergence seems not to exist in the QCDF approach even at the amplitude level.

Below we discuss the absence of the Glauber divergence at the amplitude level in QCDF in more details. The spin structure associated with the B meson wave function is written as [24,25]

$$\begin{aligned}&(P_B + m_B)\gamma_5\left[\frac{\not{n}_+}{\sqrt{2}}\phi_B^+(k) + \frac{\not{n}_-}{\sqrt{2}}\phi_B^-(k)\right]\\ &\quad = -(P_B + m_B)\gamma_5\left[\phi_B(k) - \frac{\not{n}_+ - \not{n}_-}{\sqrt{2}}\bar{\phi}_B(k)\right],\end{aligned} \tag{26}$$

with the functions

$$\phi_B = \tfrac{1}{2}(\phi_B^+ + \phi_B^-), \qquad \bar{\phi}_B = \tfrac{1}{2}(\phi_B^+ - \phi_B^-). \tag{27}$$

It has been known that only the structure $(P_B + m_B)\gamma_5\not{n}_-$ contributes to the $B \to M_1$ transition form factor, if choosing the M_1 meson momentum P_1 in the plus direction. Assuming that the same structure contributes to the nonfactorizable $B \to M_1M_2$ emission amplitude, the lower gluon vertex in Fig. 1(a) contains the matrix γ^T, since it is sandwiched by $\not{n}_- \propto \gamma^+$ from the B meson and $\not{P}_1 \propto \gamma^-$ from the M_1 meson. The upper gluon vertex must contain the matrix γ^T too. The Feynman rule involving the antiquark propagator in Fig. 1(a) then reduces to

$$\begin{aligned}&\frac{-i(\not{P}_2 - \not{k}_2 - \not{k} + \not{k}_1)}{(P_2 - k_2 - k + k_1)^2 + i\epsilon}(-ig\gamma^T)\gamma_5 P_2\\ &\quad \approx \frac{-ik_1^+\gamma^-}{2(P_2^- - k_2^- - k^-)k_1^+ + i\epsilon}(-ig\gamma^T)\gamma_5 P_2,\end{aligned} \tag{28}$$

in the collinear factorization for $P_2 \propto \gamma^+$. Canceling k_1^+ in the numerator and in the denominator, this antiquark propagator is of $O(1/m_B)$, and can be shrunk to a point in SCET. A similar argument applies to the NLO diagram Fig. 2(e), which leads to the Feynman rule

$$\begin{aligned}&\frac{-i(\not{P}_2 - \not{k}_2 - \not{k} + \not{k}_1 - \not{l})}{(P_2 - k_2 - k + k_1 - l)^2 + i\epsilon}(-ig\gamma^T)\gamma_5 P_2\\ &\quad \approx \frac{-i(k_1^+ - l^+)\gamma^-}{2(P_2^- - k_2^- - k^- - l^-)(k_1^+ - l^+) - l_T^2 + i\epsilon}\\ &\qquad \times (-ig\gamma^T)\gamma_5 P_2.\end{aligned} \tag{29}$$

The denominator becomes of $O(\Lambda^2_{\rm QCD})$ as $l^+ \to k_1^+$ and $l_T \sim O(\Lambda_{\rm QCD})$. However, this infrared region is suppressed by the numerator, so the antiquark propagator does not go on mass shell, and can be shrunk to a point. This explains why the Glauber divergence does not appear in the QCDF calculation of the nonfactorizable $B \to M_1M_2$ emission amplitudes.

If considering another spin structure $(P_B + m_B)\gamma_5\not{n}_+$ of the B meson, the lower gluon vertex in Fig. 1(a) contains the matrix γ^+, and the upper one contains γ^-. The Feynman rule involving the antiquark propagator in Fig. 1(a) then becomes

$$\begin{aligned}&\frac{-i(\not{P}_2 - \not{k}_2 - \not{k} + \not{k}_1)}{(P_2 - k_2 - k + k_1)^2 + i\epsilon}(-ig\gamma^-)\gamma_5 P_2\\ &\quad \approx \frac{-i(P_2^- - k_2^-)\gamma^+}{2(P_2^- - k_2^-)k_1^+ + i\epsilon}(-ig\gamma^-)\gamma_5 P_2,\end{aligned} \tag{30}$$

which may go on mass shell as $k_1^+ \to 0$. However, the virtual fermion propagators differ by a minus sign in Figs. 1(a) and 1(b), since the hard gluon attaches to the antiquark in M_2 in the former and to the quark in the latter. Because of the cancellation, we can neglect the spin structure $(P_B + m_B)\gamma_5\not{n}_+$ at LO. At NLO, the Feynman rule for Fig. 2(e) with the structure $(P_B + m_B)\gamma_5\not{n}_+$ is given by

$$\begin{aligned}&\frac{-i(\not{P}_2 - \not{k}_2 - \not{k} + \not{k}_1 - \not{l})}{(P_2 - k_2 - k + k_1 - l)^2 + i\epsilon}(-ig\gamma^-)\gamma_5 P_2\\ &\quad \approx \frac{-i(P_2^- - k_2^- - l^-)\gamma^+}{2(P_2^- - k_2^- - l^-)(k_1^+ - l^+) - l_T^2 + i\epsilon}(-ig\gamma^-)\gamma_5 P_2.\end{aligned} \tag{31}$$

It implies that the antiquark propagator diverges like $1/\Lambda^2_{\rm QCD}$ as $l^+ \to k_1^+$, which corresponds to the pole in

Eq. (20). The corresponding NLO correction to Fig. 1(b) is also Fig. 2(e), but with the hard gluon being on the left. In this case there is no cancellation between the NLO correction to Fig. 1(a) and the NLO correction to Fig. 1(b), and the region of $l^+ \to k_1^+$ contributes to the Glauber divergence. We postulate that the spin structure $(P_B + m_B)\gamma_5 \not{n}_+$ should be kept, and the Glauber divergence exists at the amplitude level in the QCDF calculation of the nonfactorizable emission diagrams. Note that the structure $(P_B + m_B)\gamma_5$ on the right-hand side of Eq. (26) was adopted in the PQCD approach (the contribution from the second wave function $\bar{\phi}_B$ is power suppressed [25]), and the virtual antiquark line is not shrunk to a point.

III. SOFT FACTOR FROM GLAUBER GLUONS

In this section we construct a soft factor $S(\mathbf{b})$, $\mathbf{b}$ being the impact parameter conjugate to the transverse loop momentum $\mathbf{l}_T$, which collects the Glauber gluons to all orders. The factorization at LO in the b space is trivial:

$$I_a^{(0)} = \int d^2b S^{(0)}(\mathbf{b}) \mathcal{M}_a^{(0)}(\mathbf{b}), \tag{32}$$

where the function $I_a^{(0)}$ consists of the diagrams in Fig. 1, and the LO soft factor is simply the identity, $S^{(0)}(\mathbf{b}) = 1$. The M_2 meson wave function and other subprocesses are contained in the nonfactorizable emission amplitude $\mathcal{M}_a^{(0)}$. The factorization of the soft factor at NLO has been explicitly demonstrated in Sec. II, and presented in Eq. (24), which is expressed in the b space as

$$I_a^{(1)} \approx \int d^2b S^{(1)}(\mathbf{b}) \mathcal{M}_a^{(0)}(\mathbf{b}), \tag{33}$$

with the NLO soft factor

$$S^{(1)}(\mathbf{b}) = i\frac{\alpha_s}{\pi} C_F \int \frac{d^2 l_T}{l_T^2} e^{-i\mathbf{l}_T \cdot \mathbf{b}}. \tag{34}$$

Adding the second radiative gluon emitted by the valence quark in the M_2 meson, we have

$$I_a^{(2)} \approx \frac{1}{2}\left(i\frac{\alpha_s}{\pi} C_F\right)^2 \int \frac{d^2 l_{1T} d^2 l_{2T}}{l_{1T}^2 l_{2T}^2} \mathcal{M}_a^{(0)}(\mathbf{l}_{1T} + \mathbf{l}_{2T}), \tag{35}$$

whose derivation is similar to the two-loop analysis in [11]. The above factorization implies the next-to-next-to-leading-order (NNLO) soft factor

$$S^{(2)}(\mathbf{b}) = \frac{1}{2}\left(i\frac{\alpha_s}{\pi} C_F \int \frac{d^2 l_T}{l_T^2} e^{-i\mathbf{l}_T \cdot \mathbf{b}}\right)^2. \tag{36}$$

Motivated by the above analysis up to NNLO, we postulate the all-order definition of the soft factor,

$$S(\mathbf{b}) = \langle 0 | W_+(0, \mathbf{b}; -\infty) W_+(0, \mathbf{b}; \infty)^\dagger W_-(0, \mathbf{0}_T; \infty) \times W_-(0, \mathbf{0}_T; -\infty)^\dagger | 0 \rangle, \tag{37}$$

where $\mathbf{b}$ can be interpreted as the transverse separation between the weak decay vertex and the spectator. The link W_- denotes another Wilson line operator

$$W_-(z^-, \mathbf{z}_T; \infty) = P \exp\left[-ig \int_0^\infty d\lambda n_- \cdot A(z + \lambda n_-)\right], \tag{38}$$

with the coordinate $z = (0, z^-, \mathbf{z}_T)$. The net effect of the two links $W_+(0, \mathbf{b}; -\infty) W_+(0, \mathbf{b}; \infty)^\dagger$ demands the vanishing of the component l^- of the loop momentum, and the off shellness of a Glauber gluon by l_T^2 as indicated in Eq. (23). We have included the additional link $W_-(0, \mathbf{0}; -\infty)^\dagger$ in the above definition to demand the vanishing of l^+, which plays a role similar to the antiquark propagator in M_2 for pinching the l^+ contour. It can be shown, by expanding the Wilson line operators in the coupling constant, that Eq. (37) reproduces the NLO and NNLO soft factors presented above.

We then extend the derivation of the soft factor to all orders by means of induction [14,17], and demonstrate that it leads to the operator definition in Eq. (37). Assume that the factorization holds up to $O(\alpha_s^N)$,

$$G^{(j)} = \sum_{i=0}^{j} S^{(i)} \otimes \mathcal{M}_a^{(j-i)}, \qquad j = 1, \ldots, N, \tag{39}$$

where $\otimes$ represents the convolution in b,

$$S^{(i)} \otimes \mathcal{M}_a^{(j-i)} \equiv \int d^2b S^{(i)}(\mathbf{b}) \mathcal{M}_a^{(j-i)}(\mathbf{b}). \tag{40}$$

In the above expression $S^{(i)}(\mathbf{b})$ is given by the $O(\alpha_s^i)$ terms in the perturbative expansion of Eq. (37), and $\mathcal{M}_a^{(j-i)}(\mathbf{b})$ stands for the $O(\alpha_s^{j-i})$ nonfactorizable emission amplitude. We shall show that the $O(\alpha_s^{N+1})$ diagrams $G^{(N+1)}$ can be written as the convolution of the $O(\alpha_s^N)$ diagrams $G^{(N)}$ with the $O(\alpha_s)$ soft factor by employing the Ward identity,

$$l_\mu G^\mu(l, k, k_1, k_2, \ldots) = 0. \tag{41}$$

In the above expression G^μ represents a physical amplitude with an external gluon carrying the momentum l and with n external quarks carrying the momenta $k, k_1, k_2, \ldots$. All these external particles are supposed to be on mass shell in the leading-power analysis here. It is known that factorization of a QCD process in momentum, spin, and color spaces requires summation of many diagrams. With the Ward identity in Eq. (41), the diagram summation can be handled in an elegant way.

Consider a complete set of $O(\alpha_s^{N+1})$ diagrams $G^{(N+1)}$ that are relevant to the factorization of the M_2 meson wave function. Look for the gluon, one of whose ends attaches the outermost vertex on the valence quark line in the M_2 meson. Let α denote this outermost vertex, and β denote the attachments of the other end of the identified gluon. If β is located on the valence quark line in M_2, which corresponds to a self-energy correction, and at the outer end of the valence antiquark line in M_2, which corresponds to a two-particle reducible diagram, we have Fig. 3 as the $O(\alpha_s)$ subdiagrams of $G^{(N+1)}$. In these two cases the

identified gluon can be factorized simply by inserting the Fierz transformation [17], and absorbed into the M_2 meson wave function. If β attaches to the outermost vertex of the spectator line in the B meson, we eikonalize the antiquark propagator adjacent to β into $-n_+^\beta/(n_+ \cdot l + i\epsilon)$, which has appeared in Eq. (15). Further eikonalizing the propagator of the valence quark in M_2, we factorize a piece of contribution to the NLO soft function

$$g^2 C_F \int \frac{d^4 l}{(2\pi)^4} \frac{n_-^\alpha}{n_- \cdot l + i\epsilon} \frac{-i g_{\alpha\beta}}{l^2 + i\epsilon} \frac{-n_+^\beta}{n_+ \cdot l + i\epsilon} G^{(N)}(l). \quad (42)$$

This piece can be obtained by contracting one gluon field in the Wilson line $W_-(0, \mathbf{0}_T; \infty)$ and another from $W_+(0, \mathbf{b}; -\infty)$.

For the other attachments of β to lines in $G^{(N+1)}$, we approximate the tensor $g_{\alpha\beta}$ in the propagator of the identified gluon as [17]

$$g_{\alpha\beta} \approx \frac{-n_{+\alpha} l_\beta}{-n_+ \cdot l + i\epsilon}. \quad (43)$$

The above approximation extracts the collinear enhancements associated with the energetic M_2 meson, since the lightlike vector $n_{+\alpha}$ selects the minus component of γ^α, and the dominant component $l_{\beta=+}$ in the collinear region selects the plus component of γ^β. The components $l_{\beta=-,T}$ do not affect the collinear structure, because they are negligible compared to the large momenta P_1^+ and P_2^- of $O(m_B)$. Equation (43) is applicable to the attachment to the b quark, which is free of collinear divergences. It is certainly appropriate to adopt Eq. (43) for the attachments to the internal lines and to the outer ends of the valence quark and antiquark lines in M_1, since it maintains the l^- pole structure of the propagators adjacent to the attachments. The above observation can be checked by contracting l_β to Figs. 2(b)–2(d) and 2(f), from which the conclusion in Sec. II is drawn. The only attachment of β, to which Eq. (43) does not apply, is the one to the outer end of the spectator line in the B meson, because of the wrong location of the l^- pole. This attachment has been handled separately in Eq. (42).

We have the Ward identity

$$l_\beta \Big\{ G_{\text{partial}}^{(N+1)\beta} + \Big[\bar{u}(k_2) \gamma^\beta \frac{1}{\not k_2 - \not l} \cdots \Big] + \Big[\cdots \frac{1}{\not l - \not P_2 + \not k_2} \gamma^\beta v(P_2 - k_2) \Big] + \Big[\bar{v}(k_1) \gamma^\beta \frac{1}{-\not k_1 - \not l} \cdots \Big] \Big\} = 0, \quad (44)$$

for it involves a full set of contractions of l_β to all lines in $G^{(N+1)}$. In the above expression the three diagrams with β being located at the outer ends of the valence quark and antiquark lines in M_2, and at the outer end of the spectator line in the B meson have been excluded from the set of $G_{\text{partial}}^{(N+1)}$. u and v are the spinors of a quark and an antiquark, respectively, and $\ldots$ represents the rest of Feynman rules for $G^{(N)}$. Inserting the identities

$$\begin{aligned} \bar{u}(k_2) \not l \frac{1}{\not k_2 - \not l} \cdots &= -\bar{u}(k_2) \cdots, \\ \cdots \frac{1}{\not l - \not P_2 + \not k_2} \not l v(P_2 - k_2) &= \cdots v(P_2 - k_2), \\ \bar{v}(k_1) \not l \frac{1}{-\not k_1 - \not l} \cdots &= -\bar{v}(k_1) \cdots, \end{aligned} \quad (45)$$

into Eq. (44), we derive

$$\begin{aligned} &\frac{-n_{+\alpha} l_\beta}{-n_+ \cdot l + i\epsilon} G_{\text{partial}}^{(N+1)\beta} \\ &\quad = \frac{-n_{+\alpha}}{-n_+ \cdot l + i\epsilon} [\bar{u}(k_2) \cdots - \cdots v(P_2 - k_2)] \\ &\qquad + \frac{-n_{+\alpha}}{-n_+ \cdot l + i\epsilon} \bar{v}(k_1) \cdots. \end{aligned} \quad (46)$$

The factor $-n_{+\alpha}/(-n_+ \cdot l + i\epsilon)$ in the first term on the right-hand side of Eq. (46) contributes to the Wilson lines in Eq. (1), which define the wave function for an outgoing M_2 meson.

The second term on the right-hand side of Eq. (46) contributes to another piece of the NLO soft factor,

$$g^2 C_F \int \frac{d^4 l}{(2\pi)^4} \frac{n_-^\alpha}{n_- \cdot l + i\epsilon} \frac{-i}{l^2 + i\epsilon} \frac{-n_{+\alpha}}{-n_+ \cdot l + i\epsilon} G^{(N)}(l). \quad (47)$$

Combining Eqs. (42) and (47), employing Eq. (16), working out the integrations over l^- and l^+, and Fourier transforming the NLO soft factor into the b space, we derive

$$G^{(N+1)} = S^{(1)} \otimes G^{(N)} + \mathcal{M}_a^{(N+1)}, \quad (48)$$

where $\mathcal{M}_a^{(N+1)}$ collects the $O(\alpha_s^{N+1})$ contribution that is free of the Glauber divergence. Applying the same procedure to the operator definition in Eq. (37), we obtain the similar relation for the soft factor,

$$S^{(i+1)} = S^{(1)} \otimes S^{(i)}, \quad (49)$$

for $i = 0, 1, \ldots$. At last, Eqs. (39), (48), and (49) lead to

$$\begin{aligned} G^{(N+1)} &= \sum_{i=1}^{N+1} S^{(i)} \otimes \mathcal{M}_a^{(N+1-i)} + \mathcal{M}_a^{(N+1)} \\ &= \sum_{i=0}^{N+1} S^{(i)} \otimes \mathcal{M}_a^{(N+1-i)}, \end{aligned} \quad (50)$$

with $S^{(0)} = 1$. The above expression concludes the proof for the factorization of the soft factor from the nonfactorizable emission amplitude.

IV. IMPACT ON B MESON DECAYS

In this section we investigate the numerical effect of the soft factor $S(\mathbf{b})$. The soft factor has a dynamical origin

similar to that of a meson wave function: the former (latter) absorbs the Glauber (collinear) gluons. The **b** dependence of $S(\mathbf{b})$ can be obtained by nonperturbative methods or from experimental data. For simplicity, we neglect this dependence, and parametrize the soft factor associated with $\mathcal{M}_a^{(0)}$ as $\exp(iS_e)$,

$$I_a \approx \exp(iS_e)\mathcal{M}_a^{(0)}, \tag{51}$$

where S_e is treated as a real free parameter. Glauber gluons emitted by the valence antiquark of M_2 in the LO diagram Fig. 1(b) lead to

$$I_b \approx \exp(-iS_e)\mathcal{M}_b^{(0)}, \tag{52}$$

where the minus sign is attributed to the radiation from the antiquark. In this case the right gluon in Fig. 2(e) is identified as the Glauber gluon. The above modified k_T factorization formalism with the additional soft factor also applies to the nonfactorizable emission amplitudes from other tree and penguin operators. The soft factor for a nonfactorizable annihilation amplitude is different, because Wilson lines in different directions are involved. The study of this subject will be presented elsewhere. The color-suppressed tree amplitude is small at LO due to the small Wilson coefficient a_2 for the factorizable contribution and to the pair cancellation between Figs. 1(a) and 1(b) for the nonfactorizable contribution. The presence of the soft factor can convert the destructive interference in Fig. 1 into a constructive one, resulting in strong enhancement. The soft effect is expected to be minor in amplitudes other than the color-suppressed tree, such as the color-allowed tree and penguin (including annihilation), since they receive dominant factorizable contributions.

We seek experimental constraints on the soft parameter S_e by comparing the data [3] (in units of 10^{-6})

$$\begin{aligned} B(\pi^0\pi^0) &= 1.55 \pm 0.19, \qquad [(0.29^{+0.50}_{-0.20})] \\ B(\pi^0\rho^0) &= 2.0 \pm 0.5, \qquad [\approx 0.7] \\ B(\rho^0\rho^0) &= 0.74^{+0.30}_{-0.27}, \qquad [(0.92^{+1.10}_{-0.56})], \end{aligned} \tag{53}$$

with the NLO PQCD predictions in the square brackets, which are quoted from [26], [27], and [7], respectively. The results from QCDF [6,28] are similar. The above comparison motivates us to postulate that the soft effect is significant (negligible) in the decays with M_2 being a pseudoscalar (vector) meson. That is, we associate a soft factor with $M_2 = \pi, K$, but not with $M_2 = \rho$ (the soft effect associated with the kaon is not crucial actually). A global fit to the data of the $B \to VP$ decays based on flavor $SU(3)$ symmetry also supported that the color-suppressed tree amplitude is large (small), when M_2 is a pseudoscalar (vector) meson [29]. Because the $B^0 \to \pi^0\rho^0$ decay involves both types of amplitudes with the pion and the ρ meson as M_2, it is natural that the discrepancy is in between as indicated by Eq. (53). The larger soft effect from the multiparton states in the pion than in the ρ meson can be understood by means of the simultaneous role of the pion as a $q\bar{q}$ bound state and as a Nambu-Goldstone (NG) boson [30]: the valence quark and antiquark of the pion are separated by a short distance, like those of the ρ meson, in order to reduce the confinement potential energy. The multiparton states of the pion spread over a huge spacetime in order to meet the role of a massless NG boson, which result in a strong Glauber effect.

The factorization formulas for the $B \to \pi\pi$, $\pi\rho$, πK, and ρK decays can be found in [26,31]. According to our derivation, we multiply the b quark nonfactorizable emission amplitudes, both tree and penguin, by e^{iS_e} (e^{-iS_e}) with the hard gluon being emitted by the valence antiquark (quark) in M_2. The dependence on S_e of those C-sensitive quantities is displayed in Fig. 5. The branching ratios $B(\pi^0\pi^0)$ and $B(\pi^0\rho^0)$ grow quickly with decreasing S_e from the NLO PQCD values in Eq. (53), and become close to the data when S_e reaches $-\pi/2$. Note that the Belle and *BABAR* data for $B(\pi^0\pi^0)$ have different central values, $(1.1 \pm 0.3 \pm 0.1) \times 10^{-6}$ and $(1.83 \pm 0.21 \pm 0.13) \times 10^{-6}$, respectively, and that our prediction is consistent with that of Belle. The direct CP asymmetry $A_{CP}(\pi^0 K^{\pm})$ increases from the NLO PQCD result around -0.01 [26] to above 0.05 for $S_e < -\pi/4$, whose agreement with the data $A_{CP}(\pi^0 K^{\pm}) = 0.050 \pm 0.025$ [3] is satisfactory. The deviation of the mixing-induced CP asymmetry $\Delta S_{\pi^0 K_S} \equiv S_{\pi^0 K_S} - S_{c\bar{c}s}$ descends from the NLO PQCD value $+0.07$ to -0.04 for $S_e = -\pi/2$. Compared to the data $S_{\pi^0 K_S} = 0.57 \pm 0.17$ and $S_{c\bar{c}s} = 0.672 \pm 0.024$ [3], the consistency has been improved. A measurement of sufficient accuracy with an error of better than ± 0.04 will be able to verify the predicted shift in $S_{\pi^0 K_S}$ at the 3σ level. The ratio $C/T = 0.53e^{-2.2i}$ with $S_e \approx -\pi/2$ for the $B \to \pi\pi$ decays is close to the extraction in [4], T being the color-allowed tree amplitude. An equivalent viewpoint is that the $B(\pi^0\pi^0)$ data constrain $S_e \sim -\pi/2$, which then leads to the predictions for other quantities in Fig. 5.

We have confirmed that $B(\pi^{\mp}\pi^{\pm})$, $B(\pi^0\pi^{\pm})$, and all $B(\pi K)$ change slightly from those in [26], since they are less sensitive to C. $A_{CP}(\pi^{\mp}K^{\pm})$ remains around -0.1 [1] for arbitrary S_e, and in agreement with the data $A_{CP}(\pi^{\mp}K^{\pm}) = -0.098^{+0.012}_{-0.011}$ [3]. The small variation of the curve is attributed to the soft effect on the nonfactorizable color-allowed tree and penguin contributions. $S_{\rho^0 K_S}$ does not change much, because $M_2 = \rho$ in this case, and the involved C is not modified. The NLO PQCD prediction $\Delta S_{\rho^0 K_S} \approx -0.15$ [31] is consistent with the data $S_{\rho^0 K_S} = 0.63^{+0.17}_{-0.21}$ [3]. For those penguin-dominated two-body modes without involving C, like $B \to \phi K$, their mixing-induced CP asymmetries are not affected either.

To see the uniqueness of the pion, we investigate whether the $B \to \eta'\pi^0$, $\eta'\eta'$ branching ratios exhibit a

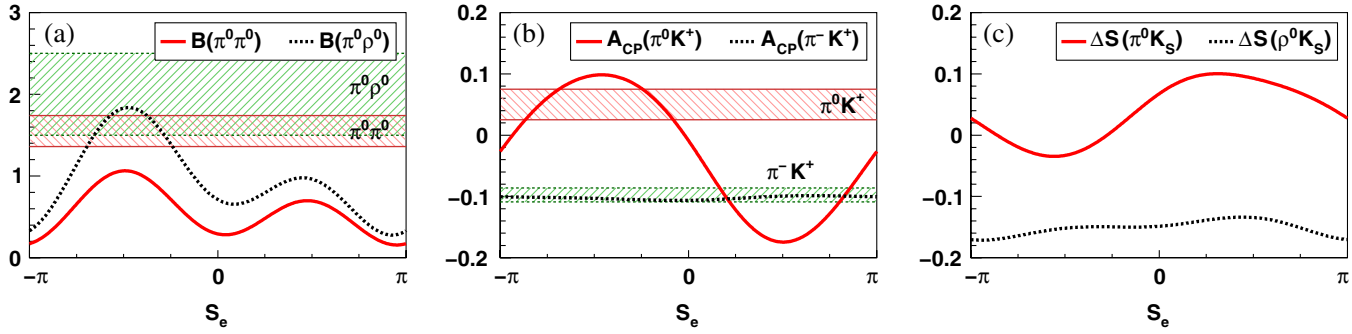

FIG. 5 (color online). S_e dependence of (a) $B(\pi^0\pi^0)$ and $B(\pi^0\rho^0)$ in units of 10^{-6}, of (b) $A_{CP}(\pi^0 K^{\pm})$ and $A_{CP}(\pi^{\mp} K^{\pm})$, and of (c) $\Delta S_{\pi^0 K_S}$ and $\Delta S_{\rho^0 K_S}$. The data (horizontal bands) for ΔS are not shown due to their large errors.

pattern similar to that of the $B \to \rho^0\pi^0, \rho^0\rho^0$ ones. The $\eta^{(\prime)}$ meson is unlikely to be a massless pseudo-NG boson because of the axial anomaly. As to $B(\eta\pi^0)$ and $B(\eta\eta)$, there are only upper bounds for their data so far. The value $B(\eta'\pi^0) = (1.2 \pm 0.4) \times 10^{-6}$ [3] has been measured, but the $B \to \eta'\eta'$ mode with $B(\eta'\eta') = [1.0^{+0.8}_{-0.6} \pm 0.1(<2.4)] \times 10^{-6}$ [32] has not yet been seen. Both $B(\eta'\pi^0)$ and $B(\eta'\eta')$ were predicted to be small in LO PQCD, roughly 0.2×10^{-6} and 0.1×10^{-6} [33], respectively. Namely, the PQCD prediction for the former is lower than the data, but that for the latter might be reasonable, a situation similar to the $B \to \rho^0\pi^0, \rho^0\rho^0$ case. We also compare the patterns of the direct CP asymmetries in the $B \to \eta^{(\prime)}K$ decays and in the $B \to \pi^0 K$ decays for the same motivation. The data $A_{CP}(\eta' K^{\pm}) = 0.016 \pm 0.019$ and $A_{CP}(\eta K^{\pm}) = -0.27 \pm 0.09$ [3] are more or less in agreement with the NLO PQCD results, -0.06 ± 0.03 and $-0.12^{+0.14}_{-0.19}$ [34], respectively. The latter value suffers from huge theoretical uncertainty, for the $B \to \eta K^{\pm}$ decays involve cancellation of two amplitudes. It seems that the $B \to \eta^{(\prime)}K$ modes behave normally, i.e., their branching ratios and CP asymmetries coincide with the PQCD predictions without the soft factor.

Our resolution differs from those based on new physics models, such as the fourth-generation model [35,36], where it is the electroweak penguin amplitude that is enhanced. These proposals, with new weak phases being introduced, change $S_{\rho^0 K_S}$ and $S_{\phi K_S}$. Our proposal differs from the elastic rescattering models for final-state interaction, which involve multiple intermediate states [37]. A large C has been generated through the charge exchange mechanism in [38]. Since the QCDF approach was employed there, the parameter scenario "S4" [6] or the inelastic scattering [39] has to be incorporated in order to get the correct result for $A_{CP}(\pi^{\mp} K^{\pm})$. The exchange mechanism, which requires turning of two energetic quarks into opposite directions, is suppressed according to the factorization theorem. Moreover, $\Delta S_{\pi^0 K_S}$ remains positive in [38].

V. CONCLUSION

In this paper we have identified the uncanceled Glauber divergences in the k_T factorization for the nonfactorizable B meson decay amplitudes, which are similar to those observed in hadron hadroproduction. The divergences are factorizable and demand the introduction of the soft factor, under which we have computed C in the PQCD approach, and found a possible simultaneous resolution of all the puzzles: $B(\pi^0\pi^0)$ and $B(\pi^0\rho^0)$ are enhanced, the difference between $A_{CP}(\pi^{\mp} K^{\pm})$ and $A_{CP}(\pi^0 K^{\pm})$ is enlarged, and $\Delta S_{\pi^0 K_S}$ is reduced for the single soft parameter S_e around $-\pi/2$. The constraint on C from the $B \to \rho\rho$ data is evaded, because of the special role of the pion as a $q\bar{q}$ bound state and as a pseudo-NG boson. Our formalism involves some assumption, so an evaluation of the **b** dependence of the soft factor, or even of the soft parameter S_e by nonperturbative methods, will shed light on the resolution proposed here. The mechanism identified in this work can be verified or falsified by more precise data in the future. Based on our observation, we agree that the $B \to \pi K$ data have not yet revealed a new physics signal [40].

ACKNOWLEDGMENTS

We thank S. Olsen and A. Soni for suggesting the investigation of the $B \to \eta^{(\prime)}K$ and the $B \to \eta^{(\prime)}\pi$ decays. We also thank M. Beneke for his useful comments. This work was supported by the National Center for Theoretical Sciences and National Science Council of R.O.C. under Grant No. NSC-95-2112-M-050-MY3.

[1] Y. Y. Keum, H-n. Li, and A. I. Sanda, Phys. Lett. B **504**, 6 (2001); Phys. Rev. D **63**, 054008 (2001).

[2] C. D. Lü, K. Ukai, and M. Z. Yang, Phys. Rev. D **63**, 074009 (2001).

[3] E. Barberio *et al.* (Heavy Flavor Averaging Group), arXiv:0808.1297.

[4] C. Chiang *et al.*, Phys. Rev. D **70**, 034020 (2004); Y. Y. Charng and H-n. Li, Phys. Rev. D **71**, 014036 (2005); R. Fleischer, S. Recksiegel, and F. Schwab, Eur. Phys. J. C **51**, 55 (2007).

[5] C. D. Lü and M. Z. Yang, Eur. Phys. J. C **23**, 275 (2002).

[6] M. Beneke and M. Neubert, Nucl. Phys. **B675**, 333 (2003).

[7] H-n. Li and S. Mishima, Phys. Rev. D **73**, 114014 (2006).

[8] R. Fleischer, S. Jager, D. Pirjol, and J. Zupan, Phys. Rev. D **78**, 111501 (2008), and references therein.

[9] M. Beneke, J. Rohrer, and D. Yang, Nucl. Phys. **B774**, 64 (2007).

[10] M. Beneke and D. Yang, Nucl. Phys. **B736**, 34 (2006); M. Beneke and S. Jager, Nucl. Phys. **B751**, 160 (2006); G. Bell, Nucl. Phys. **B795**, 1 (2008); V. Pilipp, Nucl. Phys. **B794**, 154 (2008); M. Beneke, T. Huber, and X. Q. Li, Nucl. Phys. **B832**, 109 (2010).

[11] J. Collins and J. W. Qiu, Phys. Rev. D **75**, 114014 (2007); J. Collins, arXiv:0708.4410.

[12] C. W. Bauer, B. O. Lange, and G. Ovanesyan, arXiv:1010.1027.

[13] Here a ''nonfactorizable'' amplitude refers to a contribution that does not respect the naive factorization assumption, which can also be called as a spectator amplitude.

[14] M. Nagashima and H-n. Li, Phys. Rev. D **67**, 034001 (2003).

[15] C. P. Chang and H-n. Li, arXiv:0904.4150.

[16] G. Buchalla, A. J. Buras, and M. E. Lautenbacher, Rev. Mod. Phys. **68**, 1125 (1996).

[17] H-n. Li, Phys. Rev. D **64**, 014019 (2001).

[18] X. Ji and F. Yuan, Phys. Lett. B **543**, 66 (2002); A. V. Belitsky, X. Ji, and F. Yuan, Nucl. Phys. **B656**, 165 (2003).

[19] I. O. Cherednikov and N. G. Stefanis, Phys. Rev. D **77**, 094001 (2008); Nucl. Phys. **B802**, 146 (2008).

[20] G. T. Bodwin, X. Garcia i Tormo, and J. Lee, Phys. Rev. D **81**, 114005 (2010).

[21] H-n. Li and B. Tseng, Phys. Rev. D **57**, 443 (1998).

[22] J. Chay, H-n. Li, and S. Mishima, Phys. Rev. D **78**, 034037 (2008).

[23] C. W. Bauer, D. Pirjol, and I. W. Stewart, Phys. Rev. D **67**, 071502 (2003).

[24] A. G. Grozin and M. Neubert, Phys. Rev. D **55**, 272 (1997).

[25] T. Kurimoto, H-n. Li, and A. I. Sanda, Phys. Rev. D **65**, 014007 (2001).

[26] H-n. Li, S. Mishima, and A. I. Sanda, Phys. Rev. D **72**, 114005 (2005).

[27] H-n. Li and S. Mishima (unpublished).

[28] M. Beneke, J. Rohrer, and D. Yang, Nucl. Phys. **B774**, 64 (2007); H. Y. Cheng and K. C. Yang, Phys. Rev. D **78**, 094001 (2008).

[29] C. W. Chiang and Y. F. Zhou, J. High Energy Phys. 03 (2009) 055.

[30] G. P. Lepage and S. J. Brodsky, Phys. Lett. **87B**, 359 (1979); S. Nussinov and R. Shrock, Phys. Rev. D **79**, 016005 (2009); M. Duraisamy and A. L. Kagan, Eur. Phys. J. C **70**, 921 (2010).

[31] H-n. Li and S. Mishima, Phys. Rev. D **74**, 094020 (2006).

[32] B. Aubert *et al.* (*BABAR* Collaboration), Phys. Rev. D **73**, 071102 (2006); B. Aubert *et al.* (*BABAR* Collaboration), Phys. Rev. D **74**, 051106 (2006).

[33] H. S. Wang, X. Liu, Z. J. Xiao, L. B. Guo, and C. D. Lu, Nucl. Phys. **B738**, 243 (2006); Z. J. Xiao, D. Q. Guo, and X. F. Chen, Phys. Rev. D **75**, 014018 (2007).

[34] Z. J. Xiao, Z. Q. Zhang, X. Liu, and L. B. Guo, Phys. Rev. D **78**, 114001 (2008).

[35] W. S. Hou, H-n. Li, S. Mishima, and M. Nagashima, Phys. Rev. Lett. **98**, 131801 (2007).

[36] A. Soni *et al.*, Phys. Lett. B **683**, 302 (2010).

[37] C. K. Chua, W. S. Hou, and K. C. Yang, Phys. Rev. D **65**, 096007 (2002); A. B. Kaidalov and M. I. Vysotsky, Phys. Lett. B **652**, 203 (2007); M. I. Vysotsky, arXiv:0901.2245; A. F. Falk *et al.*, Phys. Rev. D **57**, 4290 (1998).

[38] C. K. Chua, Phys. Rev. D **78**, 076002 (2008).

[39] H. Y. Cheng, C. K. Chua, and A. Soni, Phys. Rev. D **71**, 014030 (2005).

[40] M. Ciuchini *et al.*, Phys. Lett. B **674**, 197 (2009); N. Mahajan, arXiv:0812.0230.